JOURNAL OF CATALYSIS 91, 11–24 (1985)

Mössbauer Spectroscopy and Methanation Kinetics Studies of Nickel–Iron Alloy Particles Supported on Titania and Alumina

XUAN-ZHEN JIANG,[1] SCOTT A. STEVENSON, AND J. A. DUMESIC[2]

Department of Chemical Engineering, University of Wisconsin, Madison, Wisconsin 53706

Received May 4, 1984; revised August 20, 1984

Nickel–iron alloy particles (Ni : Fe = 10 : 1) were supported on titania and alumina and studied under methanation reaction conditions: temperatures from 500 to 565 K, H_2 : CO ratios from 3 to 15, and pressures near atmospheric. *In situ* Mössbauer spectroscopy was used to monitor the state of iron in these catalysts after reduction in H_2 at 713 and 773 K. For both supports, a significant fraction of the iron was alloyed with nickel after treatment in H_2, while the remainder was associated with the support as Fe^{2+}. The extent of alloy formation was greater for the titania-supported samples, indicating that iron is more reducible on titania than on alumina. Under methanation reaction conditions, some of the iron from the NiFe was oxidized to Fe^{2+}. For titania-supported samples, this process was partially reversible upon switching to H_2 at the same temperature, while the Fe^{2+} could not be re-reduced on alumina even after treatment in H_2 at 773 K. The presence of Fe^{2+} under methanation reaction conditions suggests that titanium is present as Ti^{4+}. Compared to NiFe on alumina, the titania-supported NiFe particles showed effects of "strong metal–support interactions" manifested by (i) higher methanation activity, (ii) higher activation energy and hydrogen partial pressure dependence of the methanation rate, (iii) slower deactivation under methanation reaction conditions, and (iv) greater selectivity toward higher hydrocarbons. These effects are explained by the presence of titania species (TiO_x) on the surface of the titania-supported NiFe particles. These species decrease the extent of carbon deposition on the metal surface, thereby increasing the amount of "active" carbon at the expense of "inactive" carbon. The probability of carbon chain-growth on the titania-supported NiFe particles can also be increased by addition of water to the H_2/CO feed.

INTRODUCTION

The nature of strong metal–support interactions between Group VIII metals and titania has received considerable attention in the recent literature (e.g., *1–7*). It is well-known, for example, that these interactions are induced by treatment in hydrogen at elevated temperatures (e.g., 770 K), and that these interactions suppress the chemisorption of hydrogen and carbon monoxide at room temperature. For some systems, it has also been shown that strong metal–support interactions may stabilize metal particles against sintering and may cause the metal particles to adopt a pill-box morphology (*8, 9*). The catalytic consequences of these interactions are often found to be negative, with titania-supported metals showing catalytic activities lower than those of the corresponding metals on such common supports as silica and alumina (*10*). One exception to this general trend is the methanation reaction (or more generally, Fischer–Tropsch synthesis). In particular, it has been found that Group VIII metals are more active when supported on titania, and that these catalysts may also show greater selectivities for the production of higher hydrocarbons (*11, 12*). This is especially true for the case of nickel, where titania-supported catalysts have been shown to be an order of magnitude more active for methanation than alumina-supported samples (*13, 14*). In addition, titania appears to sup-

[1] Visiting scholar from the Peoples' Republic of China, Department of Chemistry, Zhejiang University, Hangzhou, China.

[2] Author to whom correspondence should be addressed.

0021-9517/85 $3.00

press the formation of volatile nickel carbonyl in the presence of gaseous carbon monoxide (*11*).

The origin of strong metal–support interactions remains a matter of debate. It has been suggested, for example, that these interactions are due to electron transfer from reduced titania to the metal particles (e.g., *15–17*). It has been observed, however, that metal particles larger than 10 nm in size may still exhibit the effects of strong metal–support interactions, and this has led to the belief that TiO_x species may be present on the surface of the metal particles (*18–21*). Indeed, recent evidence has been reported which seems to confirm this idea (*6, 21, 22*). In general, two models have been proposed to explain the high methanation activity of titania-supported nickel catalysts. According to Vannice and Twu (*2*), strong metal–support interactions decrease the surface coverage by carbon, thereby allowing hydrogen to compete more effectively with carbon for active sites on the nickel surface. In the model of Burch and Flambard (*1*), special sites for methanation are created at the interface between the nickel particles on the titania support.

In the present paper, iron has been added to nickel particles supported on titania and alumina. Methanation reaction kinetics studies over these catalysts have been carried out to assess the importance of strong metal–support interactions for these supported NiFe particles. It will be shown accordingly that the catalytic consequences of strong metal–support interactions exhibited by NiFe supported on titania are essentially the same as those shown by supported Ni particles. In addition, Mössbauer spectroscopy has been employed to study the state of iron in these catalysts after reduction and under methanation reaction conditions. Additional characterizations of these supported NiFe catalysts using scanning transmission electron microscopy, magnetic susceptibility, and chemisorption measurements have been described elsewhere (*23*).

EXPERIMENTAL

Catalysts. Samples of nickel–iron supported on titania and alumina were prepared by incipient wetness co-impregnation using nitrate salts. The pH of the impregnation solution was adjusted to be approximately zero. Nickel loadings were typically 5 wt% on all samples, while the iron loading was about 0.5 wt%. This low loading of iron was chosen so that iron could serve as a Mössbauer spectroscopy probe of the nickel particles without dramatically altering their catalytic properties. The iron used in this study was enriched to about 90% in ^{57}Fe in order to facilitate collection of Mössbauer spectra. The details of the sample preparation procedures for these samples have been described elsewhere (*23*).

Methanation kinetics studies. Methanation kinetics studies were carried out in a 316-stainless-steel apparatus, the details of which have been described elsewhere (*24*). The reactor used for these studies operated in a down-flow geometry, with beryllium windows attached to the top and the bottom of a 1-in.-diameter tube which comprised the reactor. The operation of this reactor has been reported earlier (*25*). In short, it allows collection of reaction kinetics data and *in situ* Mössbauer spectra. These spectra are generated by passing a vertical γ-ray beam through the upper Be window, the catalyst bed in the reactor, and then out the lower Be window.

Gas phase analysis of the reactor inlet and effluent was accomplished using a SIGMA-3B gas chromatograph (Perkin-Elmer) equipped with chromosorb 102 columns. The helium carrier gas was purified by passage through a 13X molecular sieve trap at 77 K. A bed of CaC_2 was placed upstream of the detector to minimize the contribution of water in the chromatograms. Absolute calibration of the chromatograph before each run involved the averaging of three analyses of a certified standard gas mixture supplied by Matheson. The space velocities typically used

during methanation studies were ca. 1–3 × 10^5 cm^3 (STP)/g h. These values were chosen to keep the CO conversion at about 3–5% under the conditions of this study. The reaction conditions were varied over the following ranges: temperature from 510 to 570 K, pressure from 0.1 to 0.3 MPa, H_2/CO ratio from 3 to 15.

Hydrogen (National Cylinder Gases) was purified by passage through a Deoxo unit (Engelhardt) followed by an activated 13X molecular sieve trap at room temperature. Carbon monoxide (Matheson, C.P. grade) was purified by flowing it through a heated tube at 595 K, copper turnings at 595 K, and activated 3A and 13X molecular sieves at room temperature. Such a system has been shown to be effective in removing metal carbonyls from the CO stream (*24*). The purified hydrogen and carbon monoxide streams were then mixed to give the desired H_2/CO ratio, as measured by electronic mass flow meters, and fed to the reactor. In some experiments, water vapor (at pressures from ca. 3 to 27 kPa) was added to the feed by passing the synthesis gas through a water saturator located on the upstream side of the methanation reactor.

Mössbauer spectroscopy. In situ Mössbauer spectra were collected using Austin Science Associates electronics and a 1024 channel Tracor Northern multichannel analyzer, as described elsewhere (*26*). A 50 mCi source of ^{57}Co diffused into a Pd matrix was used in these measurements. Doppler velocities were calibrated with a 12.7-μm metallic iron foil and sodium nitroprusside. Isomer shifts reported in this paper have been referenced with respect to metallic iron at room temperature. All Mössbauer spectra were computer-fit using the program MFIT (*27*).

Two different sets of beryllium windows were used during the course of this study. For measurements at pressures above atmospheric, thicker (3 mm) Be windows were used, while thinner (ca. 0.1 mm) Be windows were used for measurements at atmospheric pressure. Iron is present as an impurity in these windows, and the Mössbauer spectra collected using the thicker windows show an appreciable contribution from this iron. The spectral parameters for this contribution were constrained in the computer fitting procedure to be equal to those determined from Mössbauer spectra taken of the Be windows alone (*26*). The thinner Be windows do not produce a significant iron component in the Mössbauer spectra.

RESULTS

Mössbauer Spectroscopy

In situ Mössbauer spectra collected at room temperature of the NiFe/TiO_2 sample are shown in Fig. 1. This sample contained 5.2 wt% Ni and 0.55 wt% Fe. The solid lines in this figure are the results of computer fitting. These spectra were collected using the thinner Be windows. The results of computer fitting the spectra of Fig. 1 are summarized in Table 1. The Mössbauer parameters included in this table are the isomer shift (I.S.), quadrupole splitting (Q.S.), magnetic hyperfine field (H), and the relative spectral area (A) of each component. The variation of the spectral area for reduced iron with respect to sample treatment is shown graphically in Fig. 2.

Figure 1A shows the Mössbauer spectrum after hydrogen reduction for 3 h at 713 K. The main component in this spectrum is a singlet having an isomer shift of ca.0.06 mm/s, indicative of zero-valent iron. As has been shown elsewhere (*23*), this iron is present as NiFe alloy particles. Also apparent in Fig. 1A is a weak shoulder at ca. 2 mm/s. This is due to the positive-most peak of an Fe^{2+} doublet, the second peak of which is located near zero velocity and is masked by the NiFe singlet (*28, 29*). This doublet has been attributed to ferrous cations of high coordination (e.g., octahedral) (*30*), and it will be denoted as the "outer doublet." The second shoulder in Fig. 1A, near 1 mm/s, is the positive-most peak of a doublet due to ferrous cations of low coordination (e.g., tetrahedral) or to ferric cat-

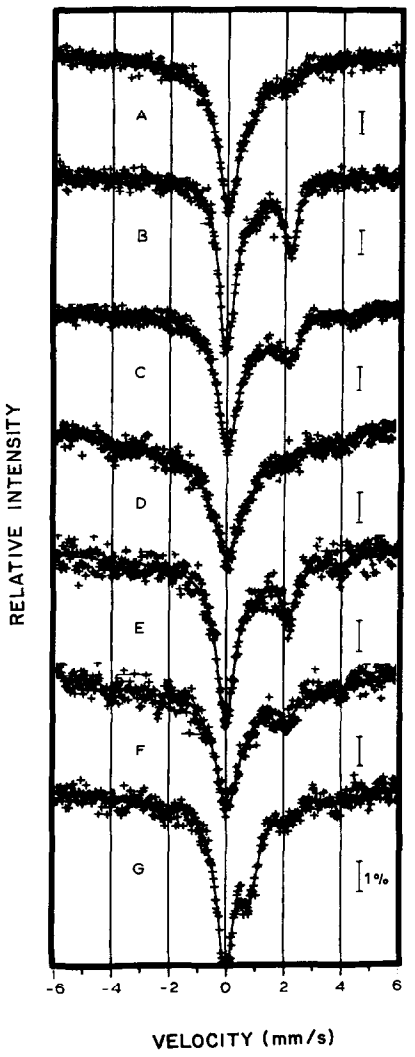

FIG. 1. Room temperature Mössbauer spectra for $NiFe/TiO_2$ after the following sequential treatments: (A) H_2, 713 K, 3 h, (B) H_2/CO = 3.3, 525 K, 1 atm, 6 h, (C) H_2, 525 K, 5 h, (D) H_2, 773 K, 2 h, (E) H_2/CO = 3.3, 525 K, 1 atm, 6 h, (F) H_2, 525 K, 5 h, (G) air at room temperature.

ions (*31*). The negative-most peak of this "inner doublet" occurs near zero velocity.

Figure 1B shows the room temperature Mössbauer spectrum obtained after subsequent treatment of the sample in H_2/CO (3.3 : 1) at atmospheric pressure and 525 K for 6 h, followed by rapid cooling (ca. 5 min) to room temperature in hydrogen. The most noticeable effect is the conversion of the NiFe spectral singlet into the ferrous outer doublet. The inner doublet also increases in intensity after this treatment. In short, exposure to synthesis gas results in the oxidation of approximately half of the zero-valent iron present in the sample. This is undoubtedly due to the H_2O and/or CO_2 formed during methanation. Upon hydrogen treatment at 525K for 5 h, a fraction of the ferrous (and possibly ferric) cations which give rise to the outer and inner doublets is reduced back to the zero-valent state, as can be seen in Fig. 1C. After subsequent reduction in hydrogen at 773 K for 2 h, essentially all of the iron is present in the zero-valent state, as evidenced in Fig. 1D by the absence of the outer and inner doublets. In addition, it is possible to see the presence of a weak six-peak pattern in the background of this figure. The positive- and negative-most peaks of this sextuplet are at ±4 mm/s, corresponding to a mag-

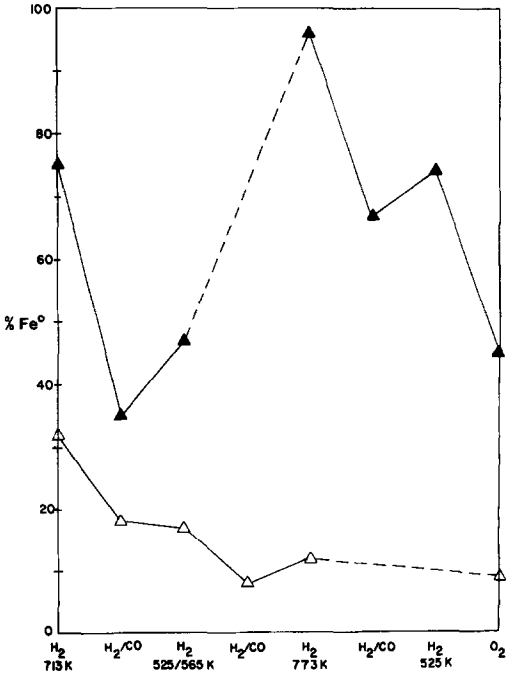

FIG. 2. Variation in percentage of iron in zero-valent state with sample treatment, calculated from the sum of the Mössbauer spectral areas of the NiFe singlet and sextuplet. (▲) $NiFe/TiO_2$, (△) $NiFe/Al_2O_3$.

TABLE 1

Mössbauer Parameters of $NiFe/TiO_2$ at 295 K

Treatment	Fe^{2+} (o.d.)			Fe^{2+} (i.d.) or Fe^{3+}			NiFe (singlet)		NiFe (sextuplet)			
	I.S. (mm/s)	Q.S. (mm/s)	Rel. area (%)	I.S. (mm/s)	Q.S. (mm/s)	Rel. area (%)	I.S. (mm/s)	Rel. area (%)	H (KOe)	I.S. (mm/s)	Q.S. (mm/s)	Rel. area (%)
a. H_2, 713 K, 3h	0.99	2.09	18	0.43	0.92	7	0.06	75	—	—	—	—
b. FTS, 525 K H_2/CO = 3.3, 6 h	1.04	2.26	45	0.51	0.87	20	0.03	35	—	—	—	—
c. FTS, 525 K H_2/CO = 3.3, 6 h H_2, 525 K, 5 h	1.07	2.12	40	0.57	1.07	13	0.04	47	—	—	—	—
d. H_2, 773 K, 2 h	1.01	2.08	3	0.49	0.90	1	0.04	65	246	0.06	0.01	31
e. FTS, 525 K H_2/CO = 3.3, 6 h	1.04	2.19	28	0.49	0.90	5	0.00	32	248	0.06	0.01	35
f. FTS, 525 K H_2, 525 K, 5 h	1.03	1.89	22	0.49	0.90	4	0.03	41	249	0.05	0.00	33
g. Exposure to air, 295 K	1.00	2.16	7	0.40	0.86	48	0.01	18	250	0.06	0.01	27

netic hyperfine field of about 245 kOe. By comparison with the work of Johnson *et al.* (*32*) on the magnetic hyperfine fields of bulk NiFe alloys, and noting that the magnetic hyperfine fields of small particles are normally smaller than those of bulk materials (*33*), it can be suggested that the iron is present as nickel-rich, NiFe alloy particles. Furthermore, the presence of both a six-peak pattern and a spectral singlet due to these NiFe particles indicates that the average size of these particles is near that for transition between superparamagnetic and ferromagnetic behavior (i.e., near 10 nm) (*33*). Analogously, the absence of a sextuplet in Fig. 1A indicates that the NiFe particles formed during reduction at 713 K are smaller than those formed during reduction at 773 K. This is in agreement with the results of chemisorption, magnetization, and electron microscopy studies of these samples, which have been reported elsewhere (*24*). Following the above reduction in hydrogen at 773 K, the sample was exposed to H_2/CO (3.3 : 1) for 6 h at 525 K, and it was then reduced in hydrogen at 525 K for 5 h. The room temperature Mössbauer spectra collected after each of these two treatments are shown in Figs. 1E and F, respectively. The changes in these spectra are similar to the changes seen in Figs. 1B and C; it is apparent that a fraction of the zero-valent iron in the sample reduced at 773 K is oxidized in H_2/CO and partially re-reduced in H_2 at 525 K. Finally, the sample was exposed to air at room temperature, during which time the iron was slowly oxidized to Fe^{3+} as shown in Fig. 1G.

Figure 3 shows room temperature Mössbauer spectra for the $NiFe/Al_2O_3$ catalyst following various treatments. This sample contained 5.8 wt.% Ni and 0.35 wt.% Fe. Table 2 gives the results of computer fitting these Mössbauer spectra. The corresponding changes in the spectral area for reduced iron versus treatment conditions are shown in Fig. 2. It can be seen from Fig. 3A that after reduction in hydrogen at 713 K, significant amounts of outer doublet, inner doublet and NiFe singlet are present. However, it is apparent from Fig. 2 that the relative amount of the NiFe singlet is smaller for this catalyst than for the titania-supported catalyst after the same treatment. Following exposure to H_2/CO (15 : 1) at atmospheric pressure and 565 K for 6 h, Fig. 3B shows that the amount of outer doublet has increased at the expense of the NiFe singlet and the inner doublet. Subsequent treatment in hydrogen at 565 K for 5 h has little effect on the Mössbauer spectrum, as seen in Fig. 3C. This is in contrast

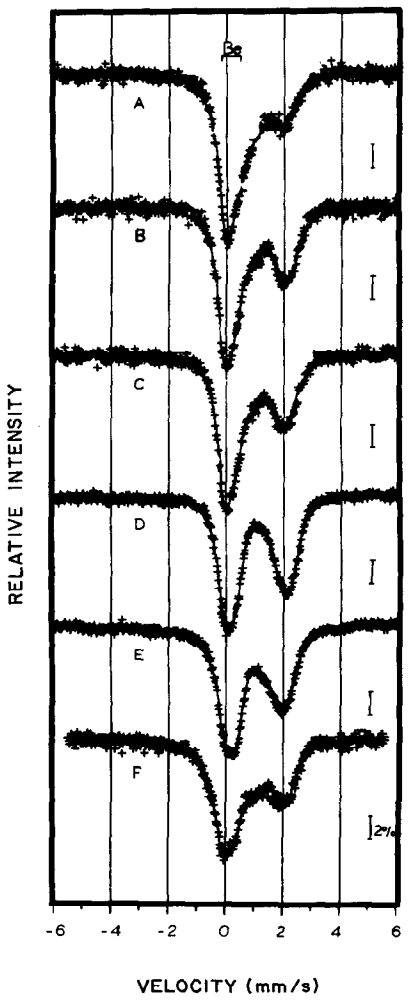

FIG. 3. Room temperature Mössbauer spectra for $NiFe/Al_2O_3$ after the following sequential treatments: (A) H_2, 713 K, 3 h, (B) H_2/CO = 15, 565 K, 1 atm, 6 h, (C) H_2, 565 K, 5 h, (D) H_2/CO = 4, 550 K, 1 atm, 6 h, (E) H_2, 773 K, 2 h, (F) air at room temperature.

to the behavior of the titania-supported catalyst, for which the outer doublet iron was partially converted to zero-valent iron during treatment in H_2 at 525 K. The observed stability of Fe^{2+} on alumina against reduction is in agreement with previous studies of low loadings of iron on this support (e.g., *25*, *29*).

At this point it is noteworthy that the treatments of the titania-supported sample in H_2/CO involved the so-called "unsafe" methanation conditions defined by Shen *et al.* (*24*). In particular, conventional nickel catalysts deactivate via nickel carbonyl formation under these conditions. For titania-supported nickel, it is possible to operate under these unsafe methanation conditions since the titania support suppresses the formation of nickel carbonyl (*11*). In the study of $NiFe/Al_2O_3$ described above, a high H_2/CO ratio was used to avoid these unsafe methanation conditions. For comparison of the alumina- and titania-supported samples, however, the $NiFe/Al_2O_3$ sample was also treated under unsafe methanation conditions, i.e., in H_2/CO (4 : 1) at 550 K and a total pressure of 0.3 MPa for 6 h. The resulting Mössbauer spectrum is shown in Fig. 3D. This spectrum is primarily composed of outer doublet, with smaller amounts of the NiFe singlet or inner doublet. Thus, the conversion of the NiFe singlet and inner doublet to the ferrous outer doublet appears to be more extensive under unsafe conditions than under safe methanation conditions. Subsequent treatment in hydrogen for 2 h at 773 K does not lead to extensive changes in the Mössbauer spectrum, as can be seen in Fig. 3E. This indicates that Fe^{2+} is more stable against reduction on Al_2O_3 than on TiO_2. Figure 3F shows that a portion of the Fe^{2+} on Al_2O_3 is oxidized to Fe^{3+} upon exposure to air at room temperature.

Methanation Kinetics

The kinetics of methanation over titania- and alumina-supported NiFe catalysts were studied over a range of reaction conditions. These data were collected under differential reactor conditions using finely divided catalyst powders to eliminate heat and mass transfer effects (*25*). For the $NiFe/TiO_2$ catalyst, the reaction temperature was varied from ca. 500 to 530 K for activation energy estimation. To determine the partial pressure dependence of the methanation rate, the hydrogen pressure was changed from 224 to 382 kPa at a constant CO pressure of 61 kPa, and the carbon monoxide pressure was varied from 23 to 75 kPa at a

TABLE 2

Mössbauer Parameters of $NiFe/Al_2O_3$ at 295 K

Treatment	Fe^{2+} (o.d.)			Fe^{2+} (i.d.) or Fe^{3+}			NiFe (singlet)	
	I.S. (mm/s)	Q.S. (mm/s)	Rel. area (%)	I.S. (mm/s)	Q.S. (mm/s)	Rel. area (%)	I.S. (mm/s)	Rel. area (%)
A. H_2, 713, 3 h	0.99	2.09	29	0.70	0.56	39	0.06	32
B. FTS, 565 K H_2/CO = 15, 6 h	1.10	1.89	65	0.57	0.79	17	−0.07	18
C. FTS, 565 K H_2/CO = 15, 6 h H_2, 565 K, 5 h	1.10	1.90	61	0.65	0.78	22	−0.06	17
D. FTS, 550 K H_2/CO = 4, 6 h	1.11	2.03	84	1.03	1.32	8	−0.03	8
E. H_2, 773 K, 2 h	1.03	1.85	83	0.86	0.86	5	0.20	12
F. Air, 295 K	1.08	1.98	46	0.63	1.10	45	−0.27	9

constant H_2 pressure of 283 kPa. The kinetic parameters derived from these measurements are summarized in Table 3. This was done for both the $NiFe/TiO_2$ sample and for a 7.4 wt% Ni/TiO_2 sample following reduction in hydrogen for 3 h at 713 K. Further kinetic measurements were made after an additional 2 h reduction treatment at 773 K.

Analogous kinetic measurements were carried out for the $NiFe/Al_2O_3$ catalyst. The reaction temperature was varied from ca. 525 to 565 K, the hydrogen pressure was changed from 247 to 385 kPa at a constant CO pressure of 24 kPa, and the carbon monoxide pressure was varied from 16 to 75 kPa at a constant H_2 pressure of 287 kPa. The results of these methanation studies are presented in Table 3. Published kinetic parameters for methanation over Ni/TiO_2 (*14*), Ni/Al_2O_3, and Fe/Al_2O_3 (*34*) are also included in Table 3 for comparison.

TABLE 3

Comparison of Kinetic Parameters for Methanation over Supported Catalysts

Catalyst	Treatment	E_m (kJ/mole)	X[a]	Y[a]
5.2% Ni / 0.55% Fe $/TiO_2$	713 K, H_2, 3 h	155	2.6	−0.8
	773 K, H_2, 2 h	187	2.4	−0.3
7.4% Ni/TiO_2	713 K, H_2, 2.5 h	93	1.2	−0.4
5.8% Ni / 0.35% Fe $/Al_2O_3$	713 K, H_2, 3 h	88	1.2	−0.6
	773 K, H_2, 2 h	102	—	—
1.53% Ni/TiO_2	Literature (*14*)	113	0.9	−0.3
5% Ni/Al_2O_3	Literature (*35*)	105	0.77	−0.31
15% Fe/Al_2O_3	Literature (*35*)	89	1.14	−0.05

[a] $r_{CH_4} = Ae^{-E_m/RT}P_{H_2}^{X}P_{CO}^{Y}$.

From Table 3 it can be seen that the activation energy for methanation over the titania-supported NiFe catalyst is higher than that over the corresponding alumina-supported sample. The reaction order with respect to hydrogen appears to be higher over $NiFe/TiO_2$ compared to $NiFe/Al_2O_3$, while the reaction order with respect to carbon monoxide is about the same on both samples.

The methanation activities of alumina- and titania-supported NiFe catalysts are given in Table 4. Activities are reported both per gram of metal and per metal surface area as measured by hydrogen desorption measurements (*20, 23*). Due to the higher activity of the titania-supported sample, it was not possible to study this catalyst at a reaction temperature of 550 K without ignition of the reactor to high conversion levels. Similarly, the alumina-supported sample was not studied at the lower temperature of 510 K to minimize the formation of nickel carbonyl. Thus, the titania- and alumina-supported catalysts are compared in Table 4 at temperatures of 510 and 550 K by suitable extrapolation using the Arrhenius equation. (Extrapolated activities are indicated by footnote *c* in Table 4.) For both samples, the activity decreases with increasing reduction temperature. In

TABLE 4

Comparison of Specific Activity for Methanation over Supported Catalysts

Catalyst	Treatment	r_{CH_4}(μmole/g metal · sec)		N_{CH_4}(sec^{-1} × 10^{+5})	
		510 K[a]	550 K[b]	510 K[a]	550 K[b]
5.2% Ni/TiO_2	713 K, H_2, 3 h	67	960[c]	30	410[c]
0.55% Fe/TiO_2	773 K, H_2, 2 h	9	230[c]	8	190[c]
5.8% Ni/Al_2O_3	713 K, H_2, 3 h	8[c]	40	3[c]	12
0.35% Fe/Al_2O_3	773 K, H_2, 2 h	—	0	—	0
7.4% Ni/TiO_2	713, H_2, 2.5 h	53	260[c]	26	130[c]

[a] Reaction condition: $H_2/CO = 4$, $P_{CO} = 61$ kPa, $T = 510$ K.
[b] Reaction condition: $H_2/CO = 4$, $P_{CO} = 61$ kPa, $T = 550$ K.
[c] Extrapolated value.

general, it can be seen that the titania-supported catalyst is more active than the alumina-supported sample, either per gram or per surface area of metal. This result is in agreement with previous studies of titania-supported nickel catalysts (*11–14*).

A further comparison of the methanation activities of the titania- and alumina-supported NiFe samples (reduced at 713 K) is shown in Fig. 4, these data being collected at or extrapolated to a temperature of 510 K, a CO pressure of 61 kPa, and an H_2/CO ratio of 4. These conditions fall in the "unsafe" methanation region defined by Shen *et al.* (*24*). The higher activity of the titania-supported catalyst is apparent in this figure. In addition, it can be seen that the alumina-supported sample deactivates more rapidly with time on stream than the titania-supported sample.

Qualitative information about the formation of higher hydrocarbons during methanation over the supported NiFe catalysts was also collected. This is presented in Table 5 for the NiFe/TiO_2 and NiFe/Al_2O_3 samples. It can be seen therein that at the low CO conversions of this study (less than ca. 5%), the selectivity is shifted toward higher hydrocarbons on the titania-supported NiFe particles. This is consistent with reported studies of Ni particles supported on titania (*11–14*).

In another series of experiments, the effect of water vapor on the rate and selectivity of methanation over the supported NiFe particles was studied. The product distributions (in mole %) for the NiFe/TiO_2 and NiFe/Al_2O_3 catalysts are shown in Table 5 for a water partial pressure of ca. 3 kPa in the H_2/CO feed. It appears that the presence of water vapor increases the produc-

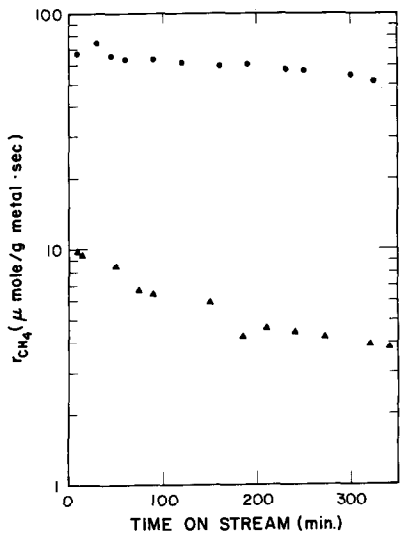

FIG. 4. Comparison of the methanation activities of NiFe/TiO_2 and NiFe/Al_2O_3 following reduction at 713 K. Methanation reaction conditions are: $H_2/CO = 4$, $P_{CO} = 61$ kPa, $T = 510$ K. (●) NiFe/TiO_2, (▲) NiFe/Al_2O_3.

TABLE 5

Product Distribution over $NiFe/TiO_2$ and $NiFe/Al_2O_3$

Catalyst and reaction condition	CO conversion (%)	CO_2	Product distribution (mol%)		
			C_1	C_2	C_3–C_5
5.8% Ni 0.35% Fe/Al_2O_3 T = 565 K, H_2/CO = 15, P_{CO} = 12 kPa	4	—	98	2	—
5.8% Ni 0.35% Fe/Al_2O_3 T = 565 K, H_2/CO = 15, P_{CO} = 12 kPa P_{H_2O} = 3 kPa	4.4	6	94	—	—
5.2% Ni 0.55% Fe/TiO_2 T = 532 K, H_2/CO = 4, P_{CO} = 30 kPa	2.3	—	58	9	33
5.2% Ni 0.55% Fe/TiO_2 T = 532 K, H_2/CO = 4, P_{CO} = 30 kPa P_{H_2O} = 3 kPa	3.8	1	43	6	50

tion of C_3–C_5 hydrocarbons for the titania-supported NiFe particles, while the effect of water on the alumina-supported NiFe catalyst is to increase slightly the production of CO_2. The dependence of the methanation rate on the water pressure over the $NiFe/TiO_2$ catalyst was studied at 525 K for a H_2 : CO ratio equal to 4, a CO pressure of 30 kPa, and a range of water partial pressures from 2.67 to 26.7 kPa. The methanation rate was observed to be inhibited slightly by water, the reaction order being −0.15. However, since selectivity to higher hydrocarbons is enhanced by the addition of water, the H_2O partial pressure dependence of the overall rate of CO consumption is slightly positive. For the $NiFe/Al_2O_3$ catalyst, the water partial pressure was varied at a temperature of 565 K, an H_2 : CO ratio of 15, and a CO pressure of 12 kPa. The rate of methanation was essentially independent of the water pressure over the range from 2.67 to 26.7 kPa.

DISCUSSION

Descriptive Model of Supported NiFe Catalysts

In general, one may imagine at least two locations for the iron in the supported NiFe catalysts of this study: (i) iron present in NiFe particles and (ii) iron interacting with the support. The formation of NiFe particles takes place during reduction of both the alumina- and titania-supported samples. The presence of iron interacting with the support is manifested by ferrous iron in the Mössbauer spectra of the alumina- and titania-supported catalysts following reduction at 713 K. This conclusion may be reached by noting that ferrous cations are stabilized against reduction to the zero-valent state on such oxide supports as SiO_2, Al_2O_3, and MgO (*28, 29, 35, 36*). It is perhaps surprising that the relative amount of ferrous iron is smaller for the titania-supported catalysts than the alumina-supported samples in this

study. That is, the iron is apparently more reducible on a reducible support such as titania than on an irreducible support such as alumina. This result is consistent with the findings of Santos *et al.* (*19*) where it was observed that low loadings (ca. 0.5 wt%) of iron on titania could be reduced to metallic iron during treatment in hydrogen at 700 K, while this is not the case for such loadings of iron on alumina or silica (*29, 35*). It has also been recently reported that nickel is highly reducible on niobia (*37*). This suggests a general result: metals may be more reducible on reducible supports than on irreducible supports.

Upon exposure to methanation reaction conditions following reduction in hydrogen, the titania- and alumina-supported catalysts showed an increase in the amount of ferrous iron at the expense of NiFe particles, indicating that a fraction of the iron in the NiFe particles becomes oxidized on both supports under methanation reaction conditions. This may be due, for example, to the presence of oxygen-containing species on the surface of the NiFe particles resulting from the dissociation of CO (*38*). Furthermore, once the ferrous cations have been formed on the $NiFe/Al_2O_3$ catalysts under "unsafe" methanation conditions, they cannot be re-reduced to the zero-valent state in hydrogen at 773 K. This is quite unlike the behavior of unsupported iron which can be reduced to the metallic state in hydrogen at temperatures near 670 K (*39*). Thus, it must be concluded that the ferrous cations formed under these methanation reaction conditions are associated with the alumina support, perhaps as a surface spinel phase (e.g., *40*). These results also suggest that bulk thermodynamics cannot necessarily be used to predict the phase of iron on these samples after various treatments. This may explain why significant amounts of Fe^{2+} were observed at the low CO conversions of this study.

It has been suggested elsewhere (*19, 20*) that the surfaces of titania-supported metal particles may contain TiO_x species which have migrated from the titania support. In an analogous way that electropositive potassium compounds have been shown to promote chemisorption of hydrogen and carbon monoxide on metals, these TiO_x species have been proposed to be electronegative and to weaken the strength of carbon monoxide adsorption on titania-supported metal particles. It is now suggested that TiO_x species may also be present on the surfaces of the NiFe particles of the present study. For example, the activation energy for methanation over the $NiFe/TiO_2$ catalysts after hydrogen treatment at 773 K is significantly higher than that over $NiFe/Al_2O_3$. This is despite the fact that the NiFe particles on titania are ca. 10 nm in size, as shown by electron microscopy, hydrogen desorption, and magnetic susceptibility measurements (*23*). As argued elsewhere (*19, 20, 22*), the observation of effects attributable to strong metal–support interactions for large metal particles is evidence for the presence of titanium species on the surfaces of these particles. In addition, the oxidation state and dispersion of these titania species may be dependent on the gas atmosphere over the sample (*18, 19*).

Catalytic Consequences of Strong Metal–Support Interactions

One important catalytic consequence of strong metal–support interactions with respect to the methanation reaction is that titania-supported nickel particles are more resistant to deactivation via nickel carbonyl migration than are alumina-supported nickel catalysts. Thus, higher catalytic activities reported for titania-supported catalysts must be viewed with caution, especially when the methanation reaction has been carried out under "unsafe" reaction conditions and when the Ni particle size has been measured before reaction kinetics studies. However, scanning transmission electron microscopy studies (*23*) indicate that while the changes in size of the alumina-supported particles under these conditions complicate the comparison of the

alumina- and titania-supported samples, it appears that the titania-supported catalysts are about an order of magnitude more active per unit surface area.

The catalytic consequences of strong metal–support interactions observed in the present study between NiFe and titania are in general agreement with the results of Vannice (*14*), who investigated a number of Group VIII metals supported on titania. In particular, the methanation activity, activation energy, reaction order with respect to hydrogen, and the selectivity to higher hydrocarbons are all greater for titania-supported NiFe compared to the alumina-based catalysts. It is suggested here that these effects may be at least partially attributable to the presence of TiO_x species on the nickel surface. These species may introduce new catalytic sites comprised of nickel and titania components, and they may alter the amount and/or nature of carbon species on the nickel surface. The first of these two possibilities is a modification of the model proposed by Burch and Flambard (*1*); the second is suggested from the arguments of Vannice (*2*). The following paragraphs discuss these two effects in greater detail.

According to Burch and Flambard (*1*), Ni/TiO_2 catalysts are more active for methanation than nickel on other common supports such as alumina due to the creation of special sites at the interface between nickel and titania. These sites were imagined to be present at the periphery of the nickel particles on the titania support. However, if the nickel particles are large, the number of these sites relative to the total metal surface area is quite small. Instead, if TiO_x species are also present on the surface of the nickel particles, then these special sites are no longer restricted to the periphery but may exist over the entire metal surface. This could explain the particularly high activity of the titania-supported methanation catalysts reported by this and other studies. These sites would presumably show a higher methanation activation energy, a higher reaction order with respect to hydrogen, and an increased selectivity toward higher hydrocarbons compared to NiFe alone; however, the reason for this behavior is not clear from this model.

The second possible role of TiO_x species on Ni (and NiFe) particles supported on titania may be to modify the amount and/or nature of the carbon species on the metal surface. It has been suggested by Vannice (*2*) that the nickel surface coverage by carbon under methanation reaction conditions may be smaller for titania-supported nickel than for nickel particles on other supports such as alumina. This allows hydrogen to compete more favorably for sites on the metal surface, and a more active methanation catalyst results (*2, 14*). It is not clear from this explanation, however, why the reaction order with respect to carbon monoxide is about the same for titania- and alumina-supported methanation catalysts. In fact, one would expect the titania-supported catalysts to show a less negative reaction order. Also, it is not apparent from this explanation why the selectivity toward higher hydrocarbons is greater for the titania-supported catalysts. For these reasons, it seems appropriate to extend the ideas of Vannice to include the possibility that titania modifies not only the amount but also the *nature* of the carbon species on the metal surface. For example, it has been shown that several different forms of carbon may exist on nickel-based catalysts (*41, 42*). These forms include carbidic carbon, graphitic carbon, amorphous carbon, and CH_x species. In fact, only a fraction of the total amount of surface carbon may be active in the methanation reaction. This fraction has been estimated to be about 10% on a typical Ni/SiO_2 methanation catalyst (*43–45*). If one simply classifies carbon species as being either "active" or "inactive" in methanation (*43*), then a possible role of TiO_x species on the surface may be to increase the relative amount of the active carbon species. Indeed, by increasing the surface concentration of active carbon species

at the expense of inactive carbon deposits, it is possible to explain the higher methanation activity and the greater selectivity toward higher hydrocarbons observed for titania-supported Ni and NiFe catalysts. In addition, the competition between active carbon and hydrogen may not be significantly altered by the presence of TiO_x species, and the reaction order with respect to carbon monoxide could, therefore, be the same for the titania- and alumina-supported catalysts.

The above explanation for the effects of strong metal–support interactions on the catalytic properties of NiFe particles is consistent with previous studies of the effects of oxygen on the catalytic properties of metal surfaces. It has been established that the presence of oxygen on or beneath metal surfaces can increase the rate of hydrocarbon synthesis from hydrogen and carbon monoxide (*44–49*). Furthermore, the extent of carbon monoxide dissociation on non-noble metals appears to be lower on surfaces containing oxygen (e.g., *50*). Thus, the role of TiO_x species on Ni and NiFe particles may be to maintain an appropriate amount of oxygen on the surface which thereby controls the extent of carbon deposition. Too high an extent of carbon deposition leads to catalyst deactivation via the formation of inactive carbon species on the metal surface (e.g., nucleation of active carbon into inactive carbon aggregates), while too low an extent would give a catalyst with a small surface concentration of active carbon species. It thus appears that this balance lies too far toward the former extreme for Ni and NiFe surfaces, and that the presence of TiO_x species on these surfaces shifts this balance toward its optimal position.

The reasons why the methanation activation energy and reaction order with respect to hydrogen are higher for NiFe supported on titania compared to the alumina-supported catalysts are not clear at present. It is possible, for example, that the activation energy is higher for the titania-supported catalysts because it is more difficult to dissociate CO on these samples. In fact, recent results suggest that the presence of TiO_x species on a nickel surface weakens the strength of CO adsorption and suppresses the dissociative adsorption of CO (*22*). The higher reaction order with respect to hydrogen for the titania-supported catalysts may possibly be due to a change in the rate-determining step or a change in the most abundant surface species. For example, the surface coverages by "active" and "inactive" carbon species discussed above may depend on the hydrogen pressure in different ways; and, if the presence of TiO_x surface species changes the relative abundance of these carbon species, the hydrogen partial pressure dependence of the rate may change accordingly.

The effects of water vapor on the selectivity toward higher hydrocarbons during methanation over $NiFe/TiO_2$ catalysts are interesting and merit further study. It has been suggested, for example (e.g., *51, 52*), that one mechanism for chain-growth during Fischer–Tropsch synthesis involves the elimination of water from OH groups on the growing carbon fragments. When water is added to the H_2/CO feed, the concentration of these OH groups would increase and the probability for chain growth would be increased accordingly. Indeed, the TiO_x species on the metal surface may well be hydroxylated in the presence of water, and these $Ti(OH)_x$ species may be the source of OH groups for the growing carbon chains. The ability of titania to dissociate water should also be noted in this respect (*53*). Another possible effect of water might be to alter the balance between "active" versus "inactive" carbon on the surface.

Finally, one may speculate whether the presence of Ti^{3+} cations is necessary for the existence of strong metal–support interactions. At least for the case of methanation, it appears that the presence of Ti^{3+} is not responsible for the catalytic behavior of titania-supported NiFe particles. Specifically, Fe^{2+} is observed by Mössbauer spec-

troscopy under methanation reaction conditions, and by thermodynamic arguments (*54*), the presence of Fe^{2+} suggests that the titanium is present as Ti^{4+}. Additional evidence that Ti^{3+} cations are not important in methanation over titania-supported NiFe is that water does not have a strong effect on the reaction, even though water would be expected to oxidize Ti^{3+} to Ti^{4+}.

In summary, the differences in catalytic properties of NiFe supported on titania compared to NiFe supported on alumina can be explained by the presence of titania species on the surface of titania-supported metal particles. These species decrease the rate of carbon deposition on the metal, thereby decreasing the amount of "inactive" carbon on the surface. This results in an increase in the amount of "active" carbon on the surface and a corresponding increase in the rate of methanation. The increased surface coverage by "active" carbon also leads to an increase in the selectivity toward higher hydrocarbons. While the titania species decrease the strength of CO adsorption on the metal surface, the strength of hydrogen adsorption may be increased (*22*). Thus, hydrogen competes more favorably with carbon monoxide for surface sites on titania-supported metals. As a result, increasing the hydrogen pressure decreases the total amount of carbon on the surface, and this may favor the formation of "active" carbon at the expense of "inactive" carbon. Accordingly, titania-supported NiFe catalysts show a high reaction order with respect to hydrogen pressure. Finally, titania species on the metal surface may serve as a source of OH groups for surface carbon species, thereby favoring chain-growth through the elimination of water between growing carbon fragments.

ACKNOWLEDGMENTS

We would like to thank the National Science Foundation for the financial support of this work. In addition, we gratefully acknowledge funding from the Chinese government which allowed one of the authors (Jiang) to be a visiting scholar at the University of Wisconsin. We are also grateful to the National Science Foundation for providing a Graduate Fellowship to another of the authors (Stevenson). Finally, we would like to thank W. M. Shen and G. B. Raupp for valuable help during the course of this study.

REFERENCES

1. Burch, R., and Flambard, A. R., *J. Catal.* **79,** 389 (1982).
2. Vannice, M. A., and Twu, C. C., *J. Catal.* **82,** 213 (1983).
3. Fung, S. C., *J. Catal.* **76,** 225 (1982).
4. Mériaudeau, P., Ellestrand, O. H., Dufaux, M., and Naccache, C., *J. Catal.* **75,** 243 (1982).
5. Mustard, D. G., and Bartholomew, C. H., *J. Catal.* **67,** 186 (1981).
6. Simoens, A. J., Baker, R. T. K., Dwyer, D. J., Lund, C. R. F., and Madon, R. J., *J. Catal.* **86,** 359 (1984).
7. Ozdogan, S. Z., Gochis, P. D., and Falconer, J. L., *J. Catal.* **83,** 257 (1983).
8. Baker, R. T. K., Prestridge, E. B., and Garten, R. L., *J. Catal.* **56,** 390 (1979).
9. Ko, E. I., and Garten, R. L., *J. Catal.* **68,** 233 (1981).
10. Burch, R., *J. Catal.* **58,** 220 (1979).
11. Vannice, M. A., and Garten, R. L., *J. Catal.* **56,** 236 (1979).
12. Bartholomew, C. H., Pannel, R. B., and Butler, J. L., *J. Catal.* **65,** 335 (1980).
13. Vannice, M. A., *J. Catal.* **66,** 242 (1980).
14. Vannice, M. A., *J. Catal.* **74,** 199 (1982).
15. Greiner, G., and Menzel, D., *J. Catal.* **77,** 382 (1982).
16. Horsley, J. A., *J. Amer. Chem. Soc.* **101,** 2870 (1979).
17. Kao, C. C., Tsai, S. C., Bahl, M. K., and Chung, Y. W., *Surface Sci.* **95,** 1 (1980).
18. Mériaudeau, P., Dutel, J. F., Dufaux, M., and Naccache, C., *Stud. Surf. Sci. Catal.* **11,** 95 (1982).
19. Santos, J., Phillips, J., and Dumesic, J. A., *J. Catal.* **81,** 147 (1983).
20. Jiang, X. Z., Hayden, T. F., and Dumesic, J. A., *J. Catal.* **83,** 168 (1983).
21. Resasco, D. E., and Haller, G. L., *J. Catal.* **82,** 279 (1983).
22. Raupp, G. B., and Dumesic, J. A., *J. Phys. Chem. Lett.* **88,** 660 (1984).
23. Jiang, X. Z., Stevenson, S. A., Dumesic, J. A., Kelly, T. F., and Casper, R. J., *J. Phys. Chem.*, in press.
24. Shen, W. M., Dumesic, J. A., and Hill, C. G., Jr., *J. Catal.* **68,** 152 (1981).
25. Shen, W. M., Dumesic, J. A., and Hill, C. G., Jr., *J. Catal.* **84,** 119 (1983).

26. Shen, W. M., Dumesic, J. A., and Hill, C. G., Jr., *Rev. Sci. Instrum.* **52,** 858 (1981).
27. Sørensen, K., "LTE. II. Internal Report No. 1," Laboratory of Applied Physics II, Technical University of Denmark, Lyngby, Denmark, 1972.
28. Raupp, G. B., and Delgass, W.N., *J. Catal.* **58,** 337 (1979).
29. Garten, R. L., and Ollis, D. F., *J. Catal.* **35,** 232 (1974).
30. Hobson, M. C., Jr., and Gager, H. M., *J. Colloid Interface Sci.* **34,** 357 (1970).
31. Blomquist, J., Csilag, S., Moberg, L. C., Larsson, R., and Rebenstorf, B., *Acta Chem. Scand., Ser. A* **33,** 515 (1979).
32. Johnson, C. E., Ridout, M. S., and Cranshaw, T. E., *Proc. Phys. Soc.* **81,** 1079 (1963).
33. Mørup, S., Dumesic, J. A., and Topsøe, H., *in* "Mössbauer Spectroscopy Applications" (R. L. Cohen, Ed.), Vol. 2, p. 1. Academic Press, New York, 1980.
34. Vannice, M. A., *J. Catal.* **37,** 449 (1975).
35. Yuen, S., Chen, Y., Kubsh, J. E., and Dumesic, J. A., *J. Phys. Chem.* **86,** 3022 (1982).
36. Boudart, M., Delbouille, A., Dumesic, J. A., Khammouma, S., and Topsøe, H., *J. Catal.* **37,** 486 (1975).
37. Ko, E. I., Hupp, J. M., Rogan, F. H., and Wagner, N. J., *J. Catal.* **84,** 85 (1983).
38. Joyner, R. W., and Roberts, M. W., *J. Chem. Soc. Faraday Trans. I* **70,** 1819 (1974).
39. Topsøe, H., Dumesic, J. A., and Boudart, M., *J. Catal.* **28,** 477 (1973).
40. Dufresne, P., Payen, E., Grimblot, J., and Bonnelle, J. P., *J. Phys. Chem.* **85,** 2344 (1981).
41. Primet, M., Dalmon, J. A., and Martin, G. A., *J. Catal.* **46,** 25 (1977).
42. McCarty, J., and Wise, H., *J. Catal.* **57,** 406 (1979).
43. Dalmon, J. A., and Martin, G. A., *in* "Proc. Seventh Inter. Congress Catal." (T. Seiyama and K. Tanabe, Eds.), p. 402. Kodansha/Elsevier, Tokyo, 1981.
44. Dalmon, J. A., and Martin, G. A., *J. Catal.* **84,** 45 (1983).
45. Biloen, P., Helle, J. N., van den Berg, F. G. A., and Sachtler, W. M. H., *J. Catal.* **81,** 450 (1983).
46. Sexton, B. A., and Somorjai, G. A., *J. Catal.* **46,** 167 (1977).
47. Dwyer, D. J., and Somorjai, G. A., *J. Catal.* **52,** 291 (1978).
48. Castner, D. G., Blackader, R. L., and Somorjai, G. A., *J. Catal.* **66,** 257 (1980).
49. van Dijk, W. L., and van der Baan, H. S., *J. Catal.* **78,** 24 (1982).
50. Bonzel, H. P., and Krebs, H. J., *Surf. Sci.* **117,** 639 (1982).
51. Vannice, M. A., *Catal. Rev. Sci. Eng.* **14,** 153 (1976).
52. Nijs, H. N., and Jacobs, P. A., *J. Catal.* **66,** 401 (1980).
53. Duprez, D., and Miloudi, A., *Stud. Surf. Sci. Catal.* **11,** 179 (1982).
54. "Heats and Free Energies of Formation of Inorganic Oxides," Bureau of Mines Bulletin 542, 1954.